Vietnam Journal of Catalysis and Adsorption
Tạp chí xúc tác và hấp phụ Việt Nam

http://chemeng.hust.edu.vn/jca/

Synthesis of WO_3/AgI photocatalysts applying for degradation of antibiotics in water

Mai Hung Thanh Tung[1], Do Minh The[2], Tran Thi Thu Hien[2], Nguyen Thi Phuong Le Chi[3], Nguyen Tri Quoc[4], Nguyen Thi Thanh Binh[2], Nguyen Vu Ngoc Mai[2], Phan Phuoc Minh Hiep[2], Nguyen Thi Dieu Cam[2]

[1] *Chemical Engineering, Ho Chi Minh City University of Food Industry, 140 Le Trong Tan, Ho Chi Minh City, Viet Nam*
[2] *Faculty of Natural Sciences, Quy Nhon University, 170 An Duong Vuong, Quy Nhon City, Binh Dinh, Viet Nam*
[3] *Hochiminh City University of Natural Resources and Environment, 236B Le Van Sy Street, Ward 1, Tan Binh District, Hochiminh City, Vietnam*
[4] *Mien Trung industry and trade college, Viet Nam, 261 Nguyen Tat Thanh, Tuy Hoa City, Phu Yen, Vietnam*
**Email: nguyenthidieucam@qnu.edu.vn*

ARTICLE INFO

Received: 05/5/2022
Accepted: 21/7/2022
Published: 25/7/2022

Keywords:

WO_3/AgI, Photocatalyst, Recombination, Amoxicillin, Visible light

ABSTRACT

In this paper, AgI was successfully synthesized in the presence of WO_3 to form AgI/WO_3 Z scheme hetero-junction by solid-phase heating method and by varying the WO_3 mole ratio (1:0.5, 1:1, 1:2 and 1:3) with respect to the AgI. The PL spectra indicate that the introduction of WO_3 to AgI can efficiently suppress the recombination of photo-generated charge carrier. The photocatalytic activity of WO_3/AgI was investigated under visible light by using the Amoxicillin (AMX) antibiotic as an organic target in aqueous solution. The WO_3/AgI photoactivity for AXM was greatly enhanced when both materials were coupled to form a Z-scheme system. The highest degradation percentage was reached using the WO_3/AgI material ratio mole of 1/1. As compared with to the pure WO_3 and AgI, the WO_3/AgI hybrid material show remarkably improved visible-induced photocatalytic activities in degrading AMX for the enhanced transport ability of electrons and holes.

Introduction

Various semiconductors have been widely studied for environmental pollution treatment, such as ZnO, TiO_2, Zn_2TiO_2, CdS, WO_3, ... [1, 2]. Among them, TiO_2 and ZnO are the most studied [2]. However, the major disadvantage of TiO_2 is its wide bandgap energy of about 3.2 eV. Therefore, the material only works in the UV light region limiting its application in the visible light region, which contains only 5% of the total photons of sunlight [3-5]. To improve the disadvantage, new potential materials with band gap in range of 1.8 - 2.8 eV would to be researched.

Various recent studies showed that silver iodide, a semiconductor, has been attracted significant attention in its application as photocatalyst to decompose organic pollutants under visible light. AgI has many advantages such as medium band gap energy of 2.78 eV [3], which has a strong ability to absorb light in the visible region to generate electrons and holes. AgI also has high reduction potential for effective reducing oxygen to $^{\bullet}O_2^-$, an intermediate radical for generation of $HO^{\bullet}$ radical decompose organic pollutants. However, AgI faces with fast recombination of photo-excited electrons and holes. To overcome this problem, scientists have applied many modification methods to

https://doi.org/10.51316/jca.2022.054

increase the photocatalytic activity of AgI such as hybridizing AgI with other materials, doping with suitable dopants [5, 16, 17].

Besides, another semiconductor containing tungsten, WO_3, has a band gap energy of about 2.8 eV and its valence band has high oxidation potential, is considerred as an ideal photocatalyst for photocatalysis under excitation of sunlight [6, 7]. Moreover, the conduction band potential of the WO_3 is lower than that of the AgI, so it is suitable to combine WO_3 and AgI to create a Z-scheme heterojunction (WO_3/AgI). Band gap energies of both AgI and WO_3 are suitable to absorb visivle light to excite electrons from their valence bands to conduction bands [8-11]. Since potential of the conduction band of WO_3 is lower than that of AgI, the photo-excited electrons on the conduction band of WO_3 would easily migrate to the valence band of the AgI and combine with its holes. The combination effectively prevents electron-hole recombination or increase electron-hole separation efficiency in each material. Thus, the WO_3/AgI hybridized system would generated signicant amount of electrons at the conduction band of the AgI and holes in the valence band of WO_3 with high redox potentials for effective reaction with O_2 and H_2O to produce $^{\bullet}OH$.

In this study, WO_3/AgI heterojunction is prepared to produce a system with a high photocatalytic activity for the removal of AMX in aqueous medium under visible light conditions.

Experimental

Photocatalyst synthesis

Synthesis of AgI material

$AgNO_3$ was added to distilled water with stirring for 1 hour at room temperature to obtain 0.2 M solution. Then, $C_6H_8O_7$ (citric acid) and KI were respectively added to the silver nitrate solution and continuously stirred for next 2 hours. The formed precipitate was separated by centrifugation before washing with distilled water. The washed sample was continuously dried at 60 ^oC for 24 hours to get AgI.

Synthesis of WO_3 material

$Na_2WO_4.2H_2O$ was mixed with citric acid $C_6H_8O_7$ (citric acid) (ratio 5:3) before dissolving in deionized water by stirring (~10 mins) to attain a clear solution, which was continuously added HCl solution (6M) to adjust pH to 1 to obtain a yellow solution. The solution was kept stirring for 30 mins before conducting hydrothermal process at 120 ^oC for 12 hours. The obtained product was washed by water to achieve neutral pH. The cleaned product was continuously calcinated at 500 ^oC for 2 hours to achieve WO_3.

Synthesis of WO_3/AgI materials

WO_3 and $AgNO_3$ were simultaneously dispersed in distilled water by stirring for 0.5 hour to get a mixture. Then, the KI solution containing citric acid was dropped to the mixture and stirring for 3 next hours. The obtained precipitate was also separated by centrifugation before washing with water. The washed sample was also dried at 60 ^oC for 24 hours to get WO_3/AgI (WA). The synthesized materials were named WA-x, which X were the mole ratios of the WO_3/AgI (X = 1/0.5 (WA-1:0.5); 1/1 (WA-1:1); 1/2 (WA-1:2); 1/3 (WA-1:3).

Characterization methods

The prepared materials were carefully analyzed by an X-ray diffractometer (D8 – Advance 5005) to investigate their microstructure. UV–vis absorption spectra of these photocatalysts have been conducted on a UV – Visible spectrophotometer (3101PC Shimadzu). Photoluminescence spectra (PL) were carried out on a Fluoromax-4-type spectrophotometer (Jobin–Yvon Co, France). Energy dispersive X-ray spectroscopy was determined on a S-4800 spectrophotometer (Hitachi – Japan). Material surfaces were characterized by scanning electronic microscopy (SEM) (JEOL JSM-6500F).

Degradation experiments

To assess the photocatalytic degradation efficiency, 0.1 g synthesized material was put in 500 mL of a 200 mL AMX (20 mg/L) stored in a dark cover beaker using as reactor. Then, the solution was constantly stirred for 120 min to get the adsorption–desorption equilibrium on photocatalyst surface. After that, the reactor was irradiated by visible light produced from 30 W (SBNL-830). At interval time of 30 minutes during photocatalysis, 5 mL suspension was withdrawn before filtrating to determine remained AMX. In detail, a mixture of NH_4OH, $NaNO_3$, C_6H_5COOH and HCl was added to the filtrated solution for complexion, which was continuously analyzied by an CE-2011, Cecil

https://doi.org/10.51316/jca.2022.054

Instruments, UV-Vis absorption spectrometer at 435 nm.

Results and discussion

Material properties

XRD patterns of the synthesized WO_3, AgI, WA-1:0.5; WA-1:1; WA-1:2 and WA-1:3 materials were shown in Fig. 1. The obtained XRD pattern of the WO_3 indicated that characteristic diffraction peaks of monoclinic WO_3 observed at 23.1 (002); 23.7 (020): 24.4 (200) and 34,1° (202) (JCPDS: 43-1035) [12-14]. The XRD diffractogram of the synthesized AgI displayed three overt diffraction peaks at 23.6; 39.1 and 46.4°, which respectively pertained to (002), (110) and (112) planes of the typical hexagonal AgI [15-17]. For WO_3/AgI composites, the XRD diffractogram of the synthesized samples exhibited wide triplet diffraction peaks at 2θ in range of 22.5 to 25. The center peak was the highest among these triplet peaks. This was due to overlap between AgI (101) and WO_3 (020) peaks.

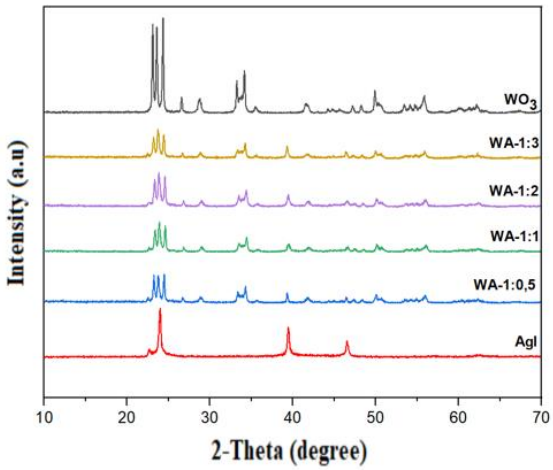

Figure 1: XRD patterns of WO_3, AgI and WA-x

The UV-Vis-DRS was carried out to investigate the optical absorption of the as-prepared samples. The UV-Vis DRS spectra of synthesized WO_3, AgI, WA-x were showed in the Fig. 2. The obtained results indicate that the AgI spectrum exhibited an edge at 456 nm, while the spectrum of the pristine WO_3 showed an edge at 445 nm. The optical absorption spectra also show that visible light absorption of the prepared WA-x materials were better than that of single WO_3 material. The WA material corresponding to 1:1 mole ratio of WO_3/AgI exhibited the highest visible light absorption among prepared composite materials. The obtained data relating to optical absorption ability were used for Kubelka-Munk equation combining with Tauc plots to estimate energy band gaps of the synthesized samples. The Tauc plots were inserted in the Fig. 3. The calculated band-gap energies of the WO_3, AgI, WA-1:0.5; WA-1:1; WA-1:2 and WA-1:3 Were 2.78; 2.73; 2.78; 2.72; 2.77 and 2.80 eV, respectively.

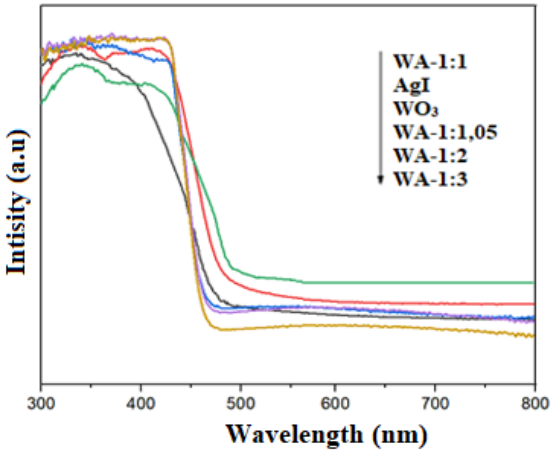

Figure 2: UV–Vis diffuse reflectance spectra of WO_3, AgI and WA-x

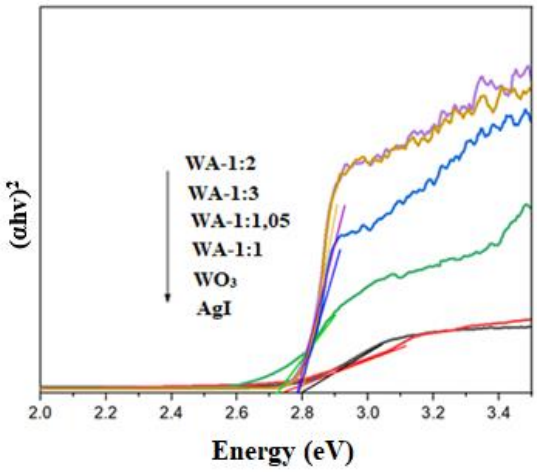

Figure 3: The plots of $(\alpha hv)^2$ versus energy (hv) for the band gap energy of AgI, WO_3 and WA-x

In PL spectra, a high peak generally attributed a quick recombination rate of electrons and holes or low charge separation efficiency while a low peak attributed to slow recombination rate or a high charge separation efficiency. The WO_3, AgI and WA-x PL spectra were shown in Fig. 4. Pure WO_3 and AgI had strong PL peak intensity. When WO_3 was combined with the AgI, the PL peak of the WA-x sample was lower than those of the AgI and WO_3 samples indicating that charge recombination of the WA was prevented. The WA-1:1 heterojunction shows a lowest luminescence emission among prepared materials.

Energy dispersive X-ray spectroscopy was used to determine the elemental composition of the

https://doi.org/10.51316/jca.2022.054

synthesized WO_3, AgI and WO_3/AgI (WA-1:1) materials in Fig. 5. The EDX spectrum of WA-1:1 indicated that the existence of W (at energy were 1.40; 1.90; 7.40; 8.40; 8.80; 9.90; 11.3; 11.6 keV), I (3.45; 3.90; 4.20; 4.80 keV), Ag (3.00 keV) and O (0.50 keV) elements without any other impurities.

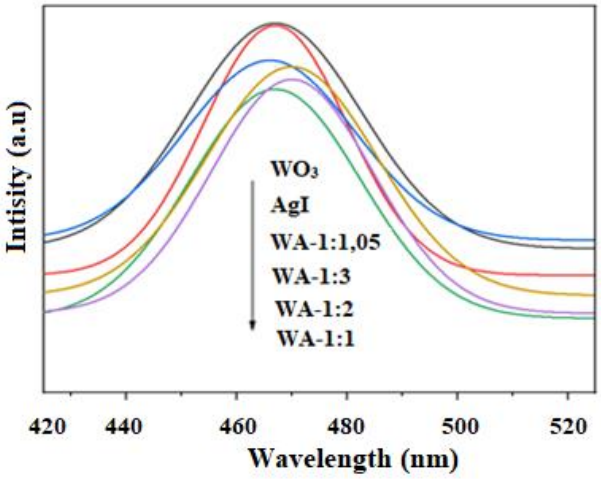

Figure 4: PL spectra of WO_3, AgI and WA-x

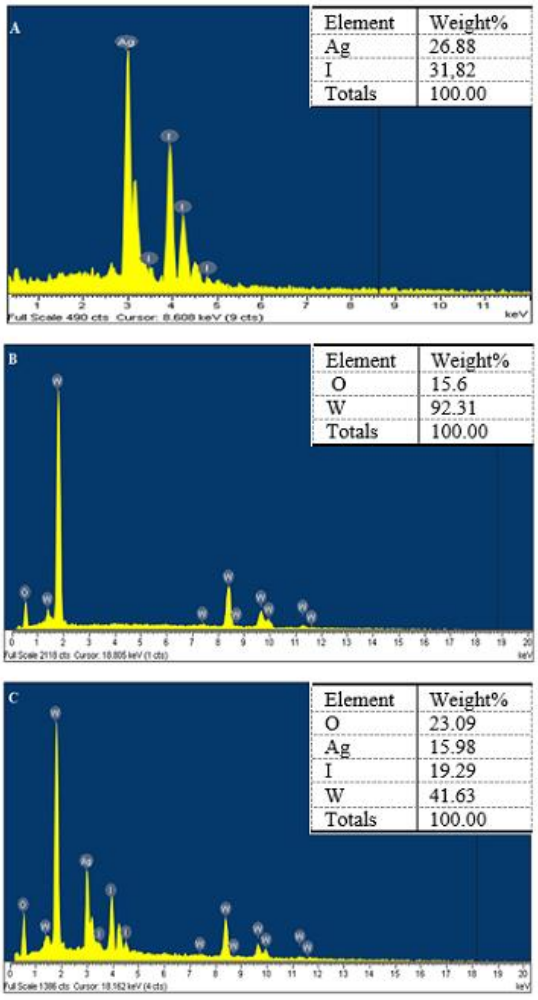

Figure 5: EDS spectra of AgI (A), WO_3 (B) and WA-1:1 (C)

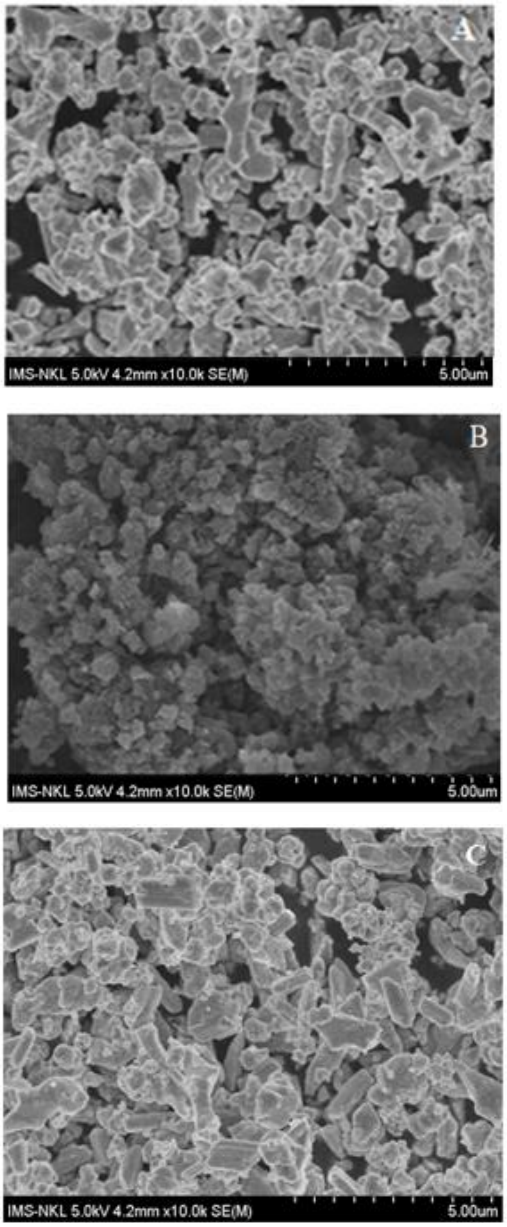

Figure 6: SEM image of AgI (a); WO_3 (b) and WA-1:1 (c)

Photocatalytic degradation

The obtained results in Fig. 7 indicates that The photocatalytic performance of WO_3/AgI were greatly higher than those of WO_3 and AgI. After 180 mins initiating by visible light, WO_3 and AgI additionally degraded 38.5 and 41.43% AMX (20 ppm), respectively. As compared to single material, the WA binary material showed a better photocatalysis for AMX degradation. In addition, the obtained enhancements in photocatalytic degradation by WO_3/AgI was increased when the with the AgI/WO_3 mole ratio increased to 1:1 (63.38%), and then became lower (the degradation performance of AMX for WA-1:2, WA-1:3, WA-1:0.5 were 50.32%, 50.02% và 47.73%,

respectively). This could be due to Z scheme mechanism in the WA, under visible light irradiation, both WO_3 and AgI could absorb photon energy to produce e^- and h^+ on their conduction band and valence band, respectively. These e^- at the conduction band would react with oxygen to produce superoxide radicals ($^{\bullet}O_2^-$) to degrade various organic compounds directly. These produced $^{\bullet}O_2^-$ would also react with water to produce hydroxyl radical ($^{\bullet}OH$), a strong oxidant, to continue degradation processes. On other hand, these left h^+ could degrade organic compounds directly or react with H_2O to generate $^{\bullet}OH$ radicals for active decomposition processes. Electrons at WO_3 conduction band could transfer to and re-combine with h^+ at AgI valence band to effectively prevent charge recombination in both WO_3 and AgI. Therefore, the WA binary heterojunction generated significant e^- and h^+ at the AgI conduction band and WO_3 valence band, respectively (Fig. 8). These charges had high redox ability to participate in photocatalysis leading to a higher AMX degradation efficiency of the WA material as compared to those of single WO_3 and AgI materials.

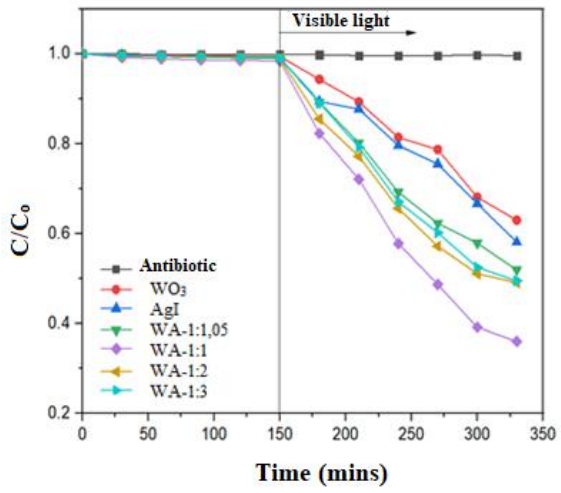

Figure 7: Conversion of AMX using WO_3, AgI and WA-x

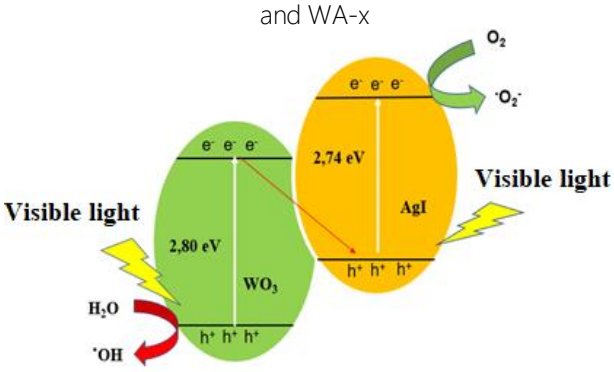

Figure 8: Amoxicillin degradation mechanism of the WO_3/AgI photocatalyst

The photocatalytic process can be represented as follows:

$$AgI + h\nu \rightarrow e_{CB}^-(AgI) + h_{VB}^+(AgI)$$

$$WO_3 + h\nu \rightarrow e_{CB}^-(WO_3) + h_{VB}^+(WO_3)$$

$$e_{CB}^-(AgI) + O_2 \rightarrow O_2^{\bullet -}$$

$$h_{VB}^+(WO_3) + H_2O \rightarrow {}^{\bullet}OH + H^+$$

$$O_2^{\bullet -} + H^+ \rightarrow HO_2^{\bullet}$$

$$e^- + HO_2^{\bullet} + H^+ \rightarrow H_2O_2$$

$$e^- + H_2O_2 + H^+ \rightarrow {}^{\bullet}OH + {}^-OH$$

$$AMX + {}^{\bullet}OH \rightarrow \text{degradation product}$$

Conclusion

We succesfully synthetized a series of WO_3/AgI heterojunctions. The WO_3/AgI photocatalysts possess significantly improved visible light photocatalytic activity for AMX degradation compared with WO_3 and AgI. The WA-1:1 (the WO_3 mole ratio with respect to the AgI was 1/1) heterojunetion exhibits the highest photocatalytic performance (the degradation efficiency of AMX is 63,38% after 180 min). Thus, the Z scheme mechanism was effectively created to induce charge generation for a novel photocatalysis to degrade AMX.

Acknowledgments

This research is funded by Ministry of Education and Training of Vietnam under grant number B2021-DQN-08.

References

1. H. Einaga, K. Mochiduki, Catalysts 3 (2013) 219–231. https://doi.org/10.3390/catal3010219
2. Mostafa Y. Nassar, Ayman A. Ali, Alaa S. Amin, RSC Advances 7 (2017) 30411. https://doi.org/10.1039/C7RA04899H
3. B. Xue, T. Sun, J. K. Wu, F. Mao, W. Yang, Ultrasonics Sonochemistry 22 (2015) 1–6. https://doi.org/10.1016/j.ultsonch.2014.04.021
4. M. Xu, J. Yang, C. Sun, Y. Cui, L. Liu, H. Zhao, B. Liang, Journal of Materials Science 56 (2020)13 2 8–1346. https://doi.org/10.1007/s10853-020-05315-w
5. M. Tang, Y. Ao, C. Wang, P. Wang, Applied Catalysis B: Environmental, 268 (2020)118395. https://doi.org/10.1016/j.apcatb.2019.118395

6. M.B. Tahir, G. Nabi, M. Rafique, N.R. Khalid, International Journal of Environmental Science and Technology 14 (2017) 2519-2542. https://doi.org/10.1016/B978-0-12-821859-4.00008-8
7. P.S. Kolhe, P.S. Shirke, N. Maiti, M.A. More, K.M. Sonawane, Journal of Inorganic and Organometallic Polymers and Materials 29 (2018) 41-48. https://doi.org/10.1007/s10904-018-0962-0
8. M. K. Arfanis, I. Ibrahim, P. Falaras, Water 11 (2019) 2439-2448. https://doi.org/10.3390/w11122439
9. L. Gao, W. Gan, Z, Qiu, X. Zhan, T. Qiang, J. Li, Scientific Reports 7 (2017) 1-13. https://doi.org/10.1038/s41598-017-01244-y
10. K. Chaudhary, N. Shaheen, S. Zulfiqar, M. I. Sarwar, M. Suleman, P. O. Agboola, I. Sharkir, M. F. Warsi, Synthetic Metals, 269 (2020) 116526. https://doi.org/10.1016/j.synthmet.2020.116526
11. Y. Wang, D. Chen, Y. Hu, L. Qin, J. Liang, X. Sun, Y. Huang, Sustainable Energy Fuels 4 (2020)1681-1692. https://doi.org/10.1039/C9SE01158G
12. X. Liu, H. Zhai, P. Wang, Q. Zhang, Z. Wang, Y. Liu, Y. Dai, B. Huang, X. Qin, X. Zhang, Environmetal Science: Nano 4 (2017) 539-557. https://doi.org/10.1039/C6EN00478D
13. M. B. Tahir, G. Nabi, M. Rafique , N. R. Khalid , International Journal of Environmental Science and Technology 14 (2017) 2519–2542. https://doi.org/10.1016/B978-0-12-821859-4.00008-8
14. T. Xiao, Z. Tang, Y. Yang, L. Tang, Y. Zhou, Z. Zou, Applied Catalysis B: Environmental 220 (2018) 417 - 428. https://doi.org/10.1016/j.apcatb.2017.08.070
15. W. Xie, L. Liu, W. Cui, W. An, Materials 12 (2019) 1-12. https://doi.org/10.3390/ma12101679
16. J. Zhang, Z. Ma, Materials Letters 216 (2018) 216–219. https://doi.org/10.1016/j.matlet.2018.01.035
17. J. Yi, L. Huang, H. Wang, H. Yu, F. Peng, Journal of Hazardous Materials, 284 (2015) 207–214. https://doi.org/10.1016/j.jhazmat.2014.11.020